Elsevier Editorial System(tm) for Microbes and Infection
Manuscript Draft

Manuscript Number: MICINF-D-15-00103R1

Title: Elucidating pathways of Toxoplasma gondii invasion in the gastrointestinal tract: Involvement of the tight junction protein occludin

Article Type: Original article

Keywords: Toxoplasma gondii; occludin; invasion; intestinal epithelial cells

Corresponding Author: Prof. simon carding, PhD

Corresponding Author's Institution: Institute of Food Research

First Author: Caroline Weight, PhD

Order of Authors: Caroline Weight, PhD; Emily Jones, BSc; Nikki Horn, BSc; Nikolaus Wellner, PhD; simon carding, PhD

Abstract: Toxoplasma gondii is an obligate intracellular parasite infecting one third of the world's population. The small intestine is the parasite's primary route of infection, although the pathway of epithelium transmigration remains unclear. Using an in vitro invasion assay and live imaging we showed that T. gondii (RH) tachyzoites infect and transmigrate between adjacent intestinal epithelial cells in polarized monolayers without altering barrier integrity, despite eliciting the production of specific inflammatory mediators and chemokines. During invasion, T. gondii co-localized with occludin. Reducing the levels of endogenous cellular occludin with specific small interfering RNAs significantly reduced the ability of T. gondii to penetrate between and infect epithelial cells. Furthermore, in vitro invasion and binding assays using recombinant occludin fragments established the capacity of the parasite to bind occludin and in particular to the extracellular loops of the protein. These findings provide evidence for occludin playing a role in the invasion of T. gondii in small intestinal epithelial cells.

Elucidating pathways of *Toxoplasma gondii* invasion in the gastrointestinal tract: Involvement of the tight junction protein occludin

Caroline M. Weight[a,c,1,2], Emily J. Jones[a,c,2], Nikki Horn[a], Nikolaus Wellner[b] and Simon R. Carding[a,c*]

[a]Gut Health and Food Safety Institute Strategic Programme and [b]Analytical Sciences Unit, Institute of Food Research, [c]Norwich Medical School, University of East Anglia, Norwich Research Park, Norwich, NR4 7UA, UK

[*]Correspondence:
Prof. SR Carding
Institute of Food Research
Norwich Research Park
Norwich, UK. NR4 7UA
(e) Simon.Carding@IFR.ac.uk
(p) +44 (0) 1603 251410

[1] Present address: Immunology Section, Leukocyte Migration Group, Department of Experimental Medicine, BMC D14, Lund University, Lund, Sweden.

[2] Authors contributed equally.

Note: Supplementary data associated with this article

Abstract

Toxoplasma gondii is an obligate intracellular parasite infecting one third of the world's population. The small intestine is the parasite's primary route of infection, although the pathway of epithelium transmigration remains unclear. Using an *in vitro* invasion assay and live imaging we showed that *T. gondii* (RH) tachyzoites infect and transmigrate between adjacent intestinal epithelial cells in polarized monolayers without altering barrier integrity, despite eliciting the production of specific inflammatory mediators and chemokines. During invasion, *T. gondii* co-localized with occludin. Reducing the levels of endogenous cellular occludin with specific small interfering RNAs significantly reduced the ability of *T. gondii* to penetrate between and infect epithelial cells. Furthermore, an *in vitro* invasion and binding assays using recombinant occludin fragments established the capacity of the parasite to bind occludin and in particular to the extracellular loops of the protein. These findings provide evidence for occludin playing a role in the invasion of *T. gondii* in small intestinal epithelial cells.

Keywords: *Toxoplasma gondii*, occludin, invasion, intestinal epithelial cells

1. Introduction

The ability of *Toxoplasma gondii* to infect almost any warm blooded animal and virtually any nucleated cell makes it the most prevalent parasitic infection worldwide. It is estimated that up to one third the world's human population is infected, although prevalence varies between countries [1, 2]. In the United States, it is estimated that approximately 22% of the population 12 years and older have been infected with *T. gondii* whereas in certain South American countries, the frequency of seropositive individuals is as high as 75% [3]. With the exception of the immunocompromised and pregnant women, *T. gondii* causes a relatively asymptomatic infection of typical fever-like symptoms. The majority of infections occur following the consumption of contaminated, undercooked meat, unwashed vegetables and contaminated water supplies [4, 5]. The gastrointestinal tract is therefore a major route of *T. gondii* infection in most cases [6, 7]. Tachyzoites are the life form of *T. gondii* that disseminate out of the gut and migrate through the body and infect the brain and muscles, where they convert to bradyzoites that form dormant, long lived and non-immunogenic cysts [8]. How the parasite transmigrates intestinal epithelial cells is unclear, although there is evidence that the paracellular pathway is important for parasite dissemination [9].

The small intestinal epithelial barrier consists of a single layer of intestinal epithelial cells (IECs) that separate the luminal contents from the underlying mucosa. These cells express apico-lateral junctional proteins, the most apical of which is the tight junction (TJ). TJs provide a barrier for the regulated passage of ions, uncharged molecules and macromolecules. They consist of a complex of over 100 proteins, the interactions of which determine barrier function. Prominent TJ proteins include the claudin family members that control permeability, junctional adhesion molecules that govern cell polarity and migration, and the MARVEL proteins such as occludin, which regulates permeability to macromolecules, while a variety of other integral membrane proteins, peripheral membrane proteins and signaling proteins such as Zonula occludens-1 (ZO-

1) make up the remaining TJ complex [10-12]. TJs are dynamic in nature and often consist of mobile pools within the membrane and cytoplasm that are involved in recycling and turnover of the protein. In the case of occludin this mobility is associated with changes in phosphorylation status [13, 14].

TJs are targeted by pathogens as a mechanism of host invasion. For example, the enteric pathogens *Vibrio cholera* and *Clostridium perfringes* secrete proteases and enterotoxins, respectively, that degrade occludin and claudins [15]. A paracellular route of entry between cells via intercellular adhesion molecule 1 (ICAM-1) by *T. gondii* has been reported [9] and we have previously shown that *T. gondii* bradyzoites and cysts affect the cellular distribution of occludin in barrier epithelial cells both *in vitro* and *in vivo* [16, 17].

Using epithelial cells derived from within the crypts of Lieberkühn of the murine small intestinal epithelium, we investigated the pathways by which *T. gondii* invades (defined as infection into cells and transmigration between cells via the paracellular pathway) the intestinal epithelium.

2. Materials and Methods

2.1 Cells.

The rodent small IEC lines m-IC_{cl2} and IEC-6 were maintained as previously described [18, 19]. To reduce occludin expression, m-IC_{c12} cells were cultured either on 13mm coverslips (for H&E staining), in 6 well plates (for immunoblotting), or on transwell cell culture inserts (for transmigration assays). In each case 0.38µg of occludin-specific siRNA (a mixture of three 19 - 25 nucleotides, Santa Cruz) in transfection media (OptiMEM, Invitrogen) was added to the cell cultures for 6 h at 37°C, washed and then incubated for a further 24 h in normal growth media. As a control, m-IC_{c12} cells were incubated with scrambled (non-silencing, scRNA) siRNAs (Santa Cruz). Occludin knockdown was assessed by immunoblotting and immunocytochemistry. Bead arrays (30 Plex Bead Mixture, BD Biosciences) were used to quantify cytokines and chemokines in cell supernatants, according to the manufacturers' instructions and analyzed using a Cytomics FC500 MPL (Beckman Coulter).

2.2 Parasites.

The type 1 RH strain of *T. gondii* tachyzoites stably expressing YFP [20] were maintained by continuous passage in confluent monolayers of Hs27 Human Fetal Foreskin Fibroblasts (European Collection of Cell Cultures) in DMEM supplemented with 2 mmol/L L-Glutamine and 10% FBS at 37C in 5% CO_2. Pelleted parasites were collected after 90% HFF lysis by centrifugation at 1000g for 15 min.

2.3 Transmigration and Infection assays.

m-IC_{cl2} cells were plated onto the apical compartment of polyethylene terephthalate (PET) cell

culture transwell inserts (8µm pore size, BD Biosciences) within a 24 well plate. TEER was measured using an Epithelial Tissue Volt Ohmmeter 2 (World Precision Instruments). By day 13, inserts contained confluent, polarized monolayers of cells. Barrier permeability was assessed by periodic TEER measurements and flux of FITC-conjugated dextran (3 - 5kDa; Sigma-Aldrich) across the transwell membrane; 1mg/ml FITC-dextran was added to the apical compartment and media from the basal compartment was analyzed for FITC content using a FLUOstar OPTIMA microplate reader (BMG Labtech). FITC-dextran quantification was determined from a standard curve generated using standards of known concentration. Transmigrating parasites were identified from the basal compartment by centrifugation and analyzing by flow cytometry using a Cytomics FC500 MPL. Data was analyzed post-collection using FlowJo version 7.6 (TreeStar).

2.4 Immunocytochemistry.

m-IC_{c12} cells were fixed in either 2% formaldehyde (to visualize the parasites) or acetone (to visualize the TJ proteins), permeabilized with 0.2% Triton X-100 and incubated with blocking buffer (0.2% Triton X-100, 3% BSA, 3% goat serum, 3% fish skin gelatin in PBS) prior to incubation with primary antibodies including occludin, claudin-2 (Invitrogen), ZO-1 (Santa Cruz) and β-catenin (BD Biosciences). Controls consisted of either no primary antibody or isotype matched antibodies of irrelevant specificity. A 1:1 mixture of Rhodamine-peanut and -wheat germ agglutinin (Vector Labs) was used to visualize the apical membrane. For transwell cultures, the PET membrane was extracted from the insert and placed cell side up onto a glass microscope slide with DePeX (BDH) and covered with a glass coverslip. To visualize intracellular parasites, m-IC_{c12} cells grown on 13mm diameter glass coverslips (BDH), fixed (2% formaldehyde), permeabilized and H&E counterstained before mounting and viewing using an upright or inverted LSM510 META on a Zeiss AxioVert 200M microscope. Images were analyzed on LSM software or AxioVision image viewer. Z stacks were composed of 1µm interval sections with the

40× objective unless stated otherwise. To visualize occludin by Z stack, cells were marked for the apical and basal membrane using surface carbohydrates and β-catenin respectively. This provided a distinction between cell domains where tight junction proteins are expressed. Throughout experiments, polarized cells were of similar depth and therefore their plane of imaging was consistent as possible. In addition, these markers provided a boundary between the membrane and cytoplasm of each cell. Image quantification was carried out using the Integrated Density tool from Image J1.47V.

2.5 Electron Microscopy.

IECs were plated onto collagen gel-coated Thermanox coverslips in 35mm dishes (Ibidi) and cultured for 8 days prior to incubation with RH-YFP *T. gondii* tachyzoites for 2 h. Media was removed and cells rinsed in PBS before fixing with 3% glutaraldehye (Agar Scientific) in 0.1M cacodylate buffer (pH 7.2) for 2 h. Further details of sample preparation can be found in the supplementary information. Samples were visualized using a Zeiss Supra 55 VP FEG SEM, operating at 3kV (Zeiss).

2.6 Two-photon-microscope live imaging.

IEC-6 were plated onto 35mm μ-dishes (Ibidi) coated with Matrigel® (Corning) and cultured for four days. Cells were labeled by staining with CellTracker™ Red CMPTX (Invitrogen) prior to apical addition of RH-YFP *T. gondii* tachyzoites immediately before imaging. Images were acquired using a LaVision BioTec TriM Scope II 2-photon microscope (Bielefeld) based on a Nikon Eclipse Ti optical inverted microscope with a Nikon 40x water immersion (Apo LWD λS NA 1.15) objective (Nikon UK Ltd) and a temperature control system (Life Imaging Services).

Multi photon excitation was provided by a Coherent Chameleon Sapphire laser (Coherent Inc.) at 1060nm to simultaneously excite CellTracker™ Red and RH-YFP *T. gondii*. Typical image volumes were 100 x 100 x 27μm and Z-stacks were separated by 1μm. Time resolved data were acquired by continuous measuring of Z-stacks for up to 30 min. The frame rate was 51.2 sec with these parameters. Images were analysed with the Fiji/ImageJ package.

2.7 Immunoblotting.

m-IC_{c12} cells were lysed in ice-cold lysis buffer (1% Triton X-100, 100 mmol/L NaCl, 25 mmol/L Tris-HCl, pH 7.4, 1 mmol/L sodium orthovanadate, 5 mmol/L EDTA, 2 mmol/L EGTA, 50 mmol/L phenylmethysulfonyl fluoride (PMSF), 25 mM sodium fluoride, 10× protease inhibitor cocktail and 15× phosphatase inhibitor cocktail (Sigma-Aldrich)) by repeatedly passing through a 19 gauge needle before centrifuging at 16,100g for 10 min at 4°C. Protein quantification was determined using the DC Protein Assay Kit (BioRad Labs). To provide additional verification of equal loading across lanes, densitometry analysis was performed on coomassie-stained gels by scanning and imaging gels using Quantity One software (version 4.6.1). For immunoblotting, samples were transferred onto Hybond C+ nitrocellulose membranes (Amersham Biosciences), blocked in 5% BSA in TTBS (150 mM NaCl, 20 mM Tris Base, 0.1% Tween-20, pH 7.4) and incubated in 1% BSA in TTBS buffer with primary antibodies for 24 h at 4°C and secondary HRP conjugates (Santa Cruz) for 1 h at 25°C. Membranes were imaged using the enhanced SuperSignal West Pico Chemiluminescent substrate (Pierce Chemical Company) and visualized with a Fluor-S-Multi Imager (Bio-Rad) and Quantity One software (version 4.5.2).

2.8 Recombinant occludin peptides.

DNA regions coding for extracellular loop (ECL) 1 (residues 85 to 138) (184bp) ECL2 (residues

191 to 241) (167bp), ECL1+ECL2 (residues 85 to 241) (485bp) and C-terminus (residues 261 to 521) (800bp) murine occludin fragments were PCR amplified from pBABE-FLAG+Occ plasmid DNA (Britta Engelhardt, University of Bern, Switzerland) [21] using the following primer pairs: ECL1-F, ATGCCATATGACACTTGCTTGGGACAG-3' and ECL1-R, 5'-AGCAGCCGGATCCTAGCCTTTGGCTGCTCTTGGGT-3' (full length ECL1); ECL2-F, 5'-ATGCCATATGATAATGGGAGTGAACCC-3' and ECL2-R, 5'-ATGGATCCTACTGGGGATCAACCACAC-3' (full length ECL2); ECL1-F, 5'-ATGCCATATGACACTTGCTTGGGACAG-3' and ECL2-R, 5'-ATGGATCCTACTGGGGATCAACCACAC-3' (full length ECL1+ECL2); and C'-F, 5'-ATGCCATATGGCTGTGAAAACCCGAAG-3' and C'-R, 5'-ATGGATCCTAAGGTTTCCGTCTG-3' (full length C-terminus). PCR products were cloned into the *Nde*I and *Bam*HI sites of the expression vector pET15b (Novagen) and sequence-verified prior to transforming *E. coli* Rosetta2 (DE3) pLysS. *E. coli* expressing His-tagged-protein products were purified using the Ni-NTA purification system (Qiagen) under denaturing conditions according to the manufacturer's instructions. Eluted proteins were immediately re-natured through the removal of urea by sequential dialysis. The purity of the recombinant occludin peptides was determined by SDS-PAGE.

3.0 Occludin-parasite binding assays.

IEC-6 cells were plated onto 13mm diameter glass coverslips (BDH) and cultured for 4 days prior to apical addition of either RH-YFP *T. gondii* tachyzoites (control) or RH-YFP *T. gondii* tachyzoites pre-incubated with 2µM recombinant occludin peptides for 15 minutes, for 2 h. To visualize intracellular parasites, IEC-6 cells were permeabilized and H&E counterstained before mounting and imaging of parasitophorous vacuoles using an inverted Zeiss AxioVert 200M microscope. Images were analyzed on AxioVision image viewer with 6-12 fields of view

recorded for each slide.

For peptide-parasite binding assays His-tagged occludin peptides or a His-tagged mCherry protein (20 µM in 6 M urea in buffer I (PBS with 1 mM CaCl and 0.05% Tween-20)) were immobilised onto Schott Nexterion H slides (Jena, Germany) of a 16-well superstructure in a humidified chamber for 2 h at 20°C. Wells were washed in decreasing concentrations of urea (4 – 0 M) in buffer I then blocking solution for 1 h (25 mM ethanolamine in 100 mM sodium borate buffer). The wells were then washed in buffer I and incubated with YFP *T. gondii* tachyzoites (10^6 per well) for 2 h at 20°C. Slides were fixed with 2% formaldehyde prior to mounting and bound parasites were visualized by UV microscopy (Zeiss AxioVert 200M microscope and AxioVision image viewer). Parasites were counted using fluorescent pixel counts at 63x magnification (Adobe Photoshop CS6) with 6-12 fields of view recorded for each well.

3.1 Statistical Analysis.

All data was assessed for normal distribution using the Kolmogarov-Smirnoff test and for homogeneity of variance by the Bartlett's test. For parametric data, an independent *t* test, or a one-way ANOVA was carried out. For non-parametric data the Mann-Whitney U test and the Kruskal-Wallis test was used. Post-Hoc analyzes were carried out with Tukey's Multiple Comparison Test or Dunn's and Dunnett's Multiple Comparison tests. Data was analyzed using Prism GraphPad software. P values of less than 0.05 were considered significant. $^{*}P<0.05$, $^{**}P<0.01$, $^{***}P<0.001$, ****P<0.0001. Any data points that were two or more standard deviations away from the mean were considered outliers and disregarded from analyzes. Error bars represent (±SEM) unless stated otherwise.

3. Results

3.1 Experimental approach.

We used a cell culture model of the mammalian intestinal epithelium to investigate how *T. gondii* interacts with and can breach the intestinal barrier. Virulent type 1 strain RH, *T. gondii* tachyzoites-YFP [20] were used in conjunction with the small intestine-derived epithelial cell lines m-IC_{cl2} [18] and IEC-6 [19] to assess barrier function, visualize and characterize parasite interactions with TJ complexes and to quantify parasite transmigration. Natural infection of *T. gondii* normally occurs via sporozoites or bradyzoites that invade the intestine and differentiate into tachyzoites. However, tachyzoites also contribute to the pathogenesis of acute toxoplasmosis [22, 23] and are infective via the oral route [24, 25, 16]. m-IC_{cl2} cells resemble those found along the of the small intestine, possessing hallmark features of cells of the lower crypt-villous axis with cytoplasmic accumulation of sucrose isomaltase, expression of the polymeric Ig receptor and cystic fibrosis transmembrane conductance regulator Cl^- channel, and the ability to produce Paneth cells [18]. IEC-6 cells possess characteristics of normal crypt epithelial cells and differentiate in culture, developing cell surface alkaline-phosphatase (ALP) enzyme activity [19, 26].

3.2 T. gondii parasites cluster around cellular junctions.

T. gondii tachyzoites dispersed over the apical surface of a confluent polarized monolayer of m-IC_{c12}, frequently settled around epithelial cellular junctions as seen by both immunofluorescence (Fig.1A, C and D) and electron microscopy (Fig.1B and E). The apical surface of cells is covered by microvilli and cell edges appear raised on SEM, which is highlighted in Fig.1B. Using TEM, parasites were observed below the apical tight junction complex (TJ, Fig.1E) and between cells (large structures above and below the parasite). This distribution of parasites suggests the paracellular pathway may be a route of infection and/or transmigration, as proposed previously

[9]. Parasites were also seen in association with the cell apical membrane, indicating multiple points of cell contact and possible docking receptors.

Using m-IC_{c12} grown on transwell inserts the number of YFP-expressing parasites transmigrating from the apical to basal compartment increased over time and up to 2 h after incubation (Fig.1F). Intracellular parasites were contained within a parasitophorous vacuole appearing as a white halo surrounding the parasite (Fig.1G). Parasite egression from infected cells was not considered an important factor within this time frame [27].

To establish whether IECs responded to *T. gondii* in this model system, cytokine and chemokine secretion was analyzed. Among those tested, significant increases in both keratinocyte chemoattractant (KC, the murine homolog of IL-8), and monocyte chemoattractant protein-1 (MCP-1) were detected in epithelial cell-conditioned media in the presence of *T. gondii* (Fig.1H). No changes in interferon-γ, interleukin (IL)-6, IL-10, IL-12, macrophage inflammatory protein (MIP)-1α, MIP-1β or tumor necrosis factor-α were detected (data not shown).

Collectively these observations reveal the ability of *T. gondii* to invade cultured IECs via infection and transmigration, with a preference for cellular boundaries as a site of epithelial cell interaction and adherence. In addition, the epithelial cells responded to the parasites via the production of specific inflammatory mediators.

3.3 T. gondii target cellular junctions and transmigrate through the epithelium via the paracellular pathway.

The route of parasite infection and transmigration was further investigated using 2-photon microscope-based live imaging. The still images taken from the video (Video S1) and shown in

Fig.1I-K illustrate the migration of YFP-*T.gondii* parasites across (I-K) and then through (I^1-K^1) the epithelial cell monolayer. Labeling of the monolayer with CellTracker™ Red emphasized the epithelial cell junctions (X plane; I-K) and paracellular space (Z plane; I^1-K^1), visible as non-stained regions between adjacent epithelial cells. The video highlights the rapid re-orientation and entry of the parasite into the paracellular space (Fig. 1J and J^1 and Video S1) in a process taking less than 52 sec. The parasite then appears to transmigrate through the monolayer, leaving the paracellular space empty (Fig. 1K and K^1 and Video S1). Paracellular egression of a parasite through the basal monolayer was also observed within minutes post-infection (data not shown).

3.4 T. gondii induces changes in the distribution of the tight junction protein occludin

Staining m-IC_{c12} cell monolayers with anti-occludin antibodies prior to and after exposure to *T. gondii* revealed that occludin localization changed over time in the presence of *T. gondii* (Fig.2). Over the time course, there was a decrease in occludin associated with the TJ complexes with staining concentrated intracellularly (Fig. 2A-E and A'-E'). This was verified by image quantification (Fig.2F and G). In detail, after 30 min, occludin appeared more concentrated at junctions compared with non-infected m-IC_{c12} cells (Fig.2B). After 2 h, the changes in occludin redistribution were more apparent, becoming apically enhanced within the cytoplasm (Fig. 2C'). Following 6 h of infection, the presence of occludin at the tight junction complex was fractured compared to the control, and was found increasingly in the cytoplasm (Fig.2D and D'). After 24 h this phenomenon was even more pronounced (Fig2.E and E'). We have also observed a similar pattern of occludin redistribution in m-IC_{cl2} cells in response to *T. gondii* (RH tachyzoite-derived) bradyzoites [17].

In summary, the immunofluorescence images demonstrate the ability of *T. gondii* to affect changes in the distribution and partitioning of occludin between the cytoplasm, cell membrane

and TJ specific domains of m-IC_{c12} epithelial cells.

3.5 T. gondii transmigrates between epithelial cells without affecting other junction-associated proteins or barrier function.

To determine if other junctional proteins were also affected by *T. gondii*, m-IC_{c12} cells were analyzed for the expression of claudin-2, ZO-1 and β-catenin. Claudin 2 is a transmembrane protein of the tight junction complex primarily involved in the regulation of permeability. ZO-1 is a scaffold protein that connects with occludin, and β-catenin is an adherens junction protein that was chosen to compare whether multiple paracellular junctions were affected by *T. gondii* in our system. In comparison to the parasite-induced redistribution of occludin, the distribution of other junctional proteins was not obviously altered upon exposure to *T. gondii* after 2 h (Fig.3A). Staining at the junctions was still apparent and unaffected by the presence of the parasite. After 6 h exposure, tight junction protein expression appeared more punctate although adherens junctions were unchanged. However, co-localization of these other proteins with *T. gondii* was not readily observed. Therefore these differences in expression may be attributed to indirect effects following changes in occludin distribution because, for example, ZO-1 interacts with occludin [28].

To determine if transmigrating parasites affected epithelial barrier integrity, transepithelial electrical resistance (TEER) and permeability were measured. After 2 h of exposure to parasites there were no significant differences in TEER (Fig.3B) or permeability to 3 – 5kDa FITC-dextran between non-infected (media) and infected m-IC_{c12} monolayers (Fig.3C). Similar findings of unaltered TEER and permeability were also seen at earlier (0.5 h) and later (6 h) intervals of parasite exposure (data not shown). These findings show that *T. gondii* tachyzoites do not adversely affect the integrity of the intestinal epithelial barrier, in agreement with previous

studies using kidney- and trophoblast-derived cell lines [9].

Immunofluorescence analysis of parasite-epithelial cell co-cultures also showed that tachyzoites co-localized with occludin which appeared to concentrate at the points of parasite entry into, or between cells (Fig.4A-E). Antibody complexes did not bind to the parasite alone (Fig.4F). After infection, occludin was localized at or in close proximity to parasites inside infected cells (Fig4.C-E and 4G-I).

3.6 T. gondii infection and transmigration through epithelial cells is reduced in cells expressing lower levels of occludin.

To determine if occludin was required for *T. gondii* infection and/or transmigration, m-IC_{c12} cells were treated for 48 h with occludin-specific small interfering RNA (siRNA) prior to incubating with parasites. Occludin knockdown was confirmed by immunoblotting with levels of reduction equating to ~35%, which persisted for up to 6 days post treatment (Fig.5A and data not shown). Treatment with occludin-specific siRNA had no effect on barrier function as determined via TEER measurements and permeability to 3 - 5kDa dextran (Fig.5B-C). Immunofluorescent staining of siRNA-treated cells confirmed reduced levels of occludin in cells treated with occludin-specific siRNA (Fig.5H) and showed that occludin-specific siRNA had no discernable off-target effects as evidenced by expression of other TJ proteins including claudin-2, ZO-1 and β-catenin that was unaffected by the siRNA treatment (Fig. 5I-K).

To determine whether or not expression levels of occludin were important for the attachment, invasion and transmigration of *T. gondii*, m-IC_{c12} cells treated with siRNAs against occludin were incubated with parasites. As the parasitophorous vacuole in infected cells is impermeable to H&E it is possible to quantify the numbers of extracellular (adhered, Fig.5D) and intracellular parasites

(Fig.5E) using H&E stained preparations of IECs. In cells with reduced levels of occludin there was a modest but significant decrease in the number of adherent parasites (Fig.5D), which correlated with a significant decrease in the proportion of cells infected by *T. gondii* compared to cells treated with non-silencing siRNAs (Fig.5E). In addition, significantly fewer transmigrating parasites were detected in occludin siRNA-treated cells compared to non-silencing siRNA-treated cells (Fig.5F) despite the number of apical parasites present in each sample being equivalent (Fig.5G).

Following exposure to *T. gondii*, residual occludin in occludin siRNA-treated cells was redistributed in a similar way to that seen in non-treated or non-silencing siRNA-treated cells (Fig.5H), suggesting that *T. gondii* was still able to interact with the residual occludin. By contrast, there were no changes in the distribution of other junctional proteins following infection of occludin-reduced cells (Fig.5I-K).

3.7 T. gondii binds the extracellular loops of occludin.

To determine *T. gondii* tachyzoite interactions with occludin, an *in vitro* infection assay was developed to assess changes in cellular attachment. As the extracellular loops (ECLs) of occludin bind to each other on adjacent cells [29, 30] we speculated that this part of the molecule is most likely to be accessible to interact with *T. gondii* in the paracellular space. Prior to infection of IEC-6, *T. gondii* tachyzoites were pre-incubated with occludin peptides (ECL2, amino acid residues 191 to 241; ECL1+ECL2, residues 85 to 241 and, as a control, C-terminus residues 261 to 521, (Fig.6A-B). Extracellular, attached parasites were identified by the absence of a intracellular parasitophorous vacuoles. Pre-incubation of *T. gondii* pre-incubation with the ECL1+ECL2 and to a lesser extent the C-terminus peptide, significantly reduced attachment to

the epithelial cells (Fig. 7A), suggesting *T. gondii* tachyzoites physically interact with the ECL1+2 and C-terminus peptides, which blocks parasite attachment to IEC-6.

To determine if occludin and *T. gondii* tachyzoites can physically interact, a solid phase *in vitro* binding assay was developed. YFP-parasites were incubated in individual wells of a modified microscope chamber slide to which occludin peptides (ECL1, amino acid residues 85 to 138; ECL2, amino acid residues 191 to 241; ECL1+ECL2, residues 85 to 241 and, as a control, C-terminus residues 261 to 521, (Fig.6A-B) were immobilized. The images in Fig.7B show the aggregation and clustering of large numbers of parasites in wells containing the ECLl+ECL2 occludin peptide. This contrasted with the low density of parasites randomly scattered across wells containing the C-terminus peptide, or in control wells containing an irrelevant protein (mCherry) or, peptide-binding media alone. Image quantification of bound parasites showed that the highest levels of bound parasites were in wells coated with the ECL1+ECL2 and ECL1 peptides, suggesting that *T. gondii* tachyzoites can bind the extracellular loops of occludin and in particular, to ECL1 (Fig.7C).

4. Discussion

Here, we provide evidence of the ability of *T. gondii* tachyzoites to access the paracellular pathway as a means of invading and transmigrating polarized intestinal epithelial cell monolayers. We have also presented evidence indicating a physical interaction can occur, at least *in vitro*, between *T. gondii* and intestinal epithelial TJ complexes via occludin. Ingested parasites (sporozoites in oocysts and bradyzoites in tissue cysts) invade the intestine and differentiate into tachyzoites, followed by the spread of the organisms hematogenously and via lymphatics [8]. Our studies on the mechanism of epithelial cell transmigration by *T. gondii* tachyzoites are, we believe,

relevant to the role this stage plays in host infection and dissemination across boundary epithelial cells. Occludin may therefore be a modulator of parasite transmigration via the paracellular pathway.

Many enteric pathogens have evolved mechanisms for targeting TJ-associated proteins for invasion. Alterations in the distribution or integrity of occludin are associated with infection of IECs by pathogens that cause gastroenteritis including *Salmonella* typhimurium [31] and enteropathogenic *E. coli* [32]. Whether or not other infectious life stages of *T. gondii* and the slow cyst-forming bradyzoite stage that is mostly associated with natural infections [33], also target the paracellular pathway, remains to be determined. Of relevance, we have shown that bradyzoites derived from the YFP-expressing RH tachyzoites used in this study also induce alterations in occludin distribution in m-IC_{cl2} epithelial cells [17]. However, in contrast to tachyzoite invasion, bradyzoites caused an increase in epithelial permeability. As bradyzoites contain different surface antigens to tachyzoites it is probable that there are multiple antigens and proteins the parasites use to infect different cells [34].

The redistribution of occludin in IECs exposed to *T. gondii* was seen across the epithelial cell monolayer despite only a proportion of infected cells. This dichotomy could result from direct and transient contact with parasites [35]. Alternatively, infected cells secrete cytokines and chemokines in response to pathogen exposure that may act upon neighboring cells and TJ complexes in a paracrine fashion [36-38].

The reduction of cellular occludin following siRNA treatment decreased transmigration by ~65%, but only decreased invasion by ~20%. Occludin may therefore be of more importance for the transmigration of *T. gondii* rather than invasion of IECs. Alternatively, changes in paracellular macromolecular flux, which is in part regulated by occludin, could also affect transmigration rates

[12, 29]. Without inhibitory occludin antibodies recognizing the extracellular domains, it was not possible to perform competition or neutralizing assays as a complimentary approach to quantify parasite transmigration between or infection into IECs. The decrease in attachment and infection following the partial reduction of occludin expression indicates that occludin may also be required for *T. gondii* to enter epithelial cells.

The identity of parasite-derived occludin binding partners was not established here. Preliminary data from immunoprecipitation and mass spectrometry analyses reveals parasite microneme and dense granule proteins to be associated with occludin (data not shown). Given that *T. gondii* is capable of invading most cell types, it is perhaps surprising that only a few cell surface receptors and *T. gondii* ligands have so far been identified. Amongst these, *T. gondii* can attach via GPI-anchored membrane proteins (e.g. SAG1) to host glucosamine receptors [39], and to galectin-like molecules on the cell surface [40], which assist in the formation of the microneme MIC1-MIC6 protein complex that is secreted during infection [41]. MIC2 binds to ICAM-1 on the surface of IECs and this interaction is considered important for parasite transmigration [9]. Sulfated glycosaminoglycans (GAGs), heparin sulfated proteoglycans and sialic acid residues on host cells have also been shown to mediate binding and invasion of *T. gondii* [42-44]. These molecules represent possible adherence receptors on IECs that the parasite can manipulate before migrating to the lateral junctions.

After 24 h of infection, IECs contained multiple parasites that remain co-localized with occludin. Peptides of ECL1 and ECL2 can increase the rate of occludin turnover and as *T. gondii* binds the extracellular loops of occludin, it is possible that endocytosis of occludin may occur following interactions with the parasite [45, 46]. This could explain why after 24 h of infection the concentration of cellular occludin was increased compared to non-infected cells. Increased rates of recycling are also thought to be a common mechanism in pathogen invasion [47]. Alternatively,

there may be increased synthesis of occludin, which was not addressed in this study. The results of our occludin binding assay suggest that *T. gondii* may associate with ECL1. This loop contains a high percentage of tyrosine and glycine residues that are thought to provide flexibility to the molecule, which also possesses self-associating properties [30].

In summary, we have provided evidence of *Toxoplasma gondii* tachyzoites targeting the paracellular pathway as a means of transmigrating epithelial cell monolayers in a process that appears to involve interactions with occludin. These findings have implications for understanding how *T. gondii* invades its host and further highlights the susceptibility of the intestinal epithelial barrier to pathogens that target the most apical junctional complexes.

Acknowledgements

The work was supported by an Institute Strategic Programme Grant IFR/08/1 and PhD studentships from the BBSRC (CMW; BB/D526488/1) and UEA (EJJ). The authors are grateful to Dr. Kathryn Cross and Dr. Mary Parker for assistance with EM at the Analytical Sciences Unit, Dr. Duncan Gaskin for assistance in the development the occludin-parasite binding assay, at the Institute of Food Research, UK, and Dr. Britta Engelhardt, University of Bern, Switzerland for providing the pBABE-FLAG+Occ plasmid.

Conflict of Interest

The authors declare no conflicts of interest.

References

[1] Weiss LM, Dubey JP. Toxoplasmosis: A history of clinical observations. Int J Parasitol 2009;39:895-901.

[2] Sukthana Y. Toxoplasmosis: beyond animals to humans. Trends Parasitol 2006;22:137-42.

[3] Montoya JG, Liesenfeld O. Toxoplasmosis. Lancet 2004;363:1965-76.

[4] Jones JL, Dubey JP. Waterborne toxoplasmosis - Recent developments. Exp Parasitol 2010;124:10-25.

[5] Jones JL, Dubey JP. Foodborne toxoplasmosis. Clin Infect Dis 2012;55:845-51.

[6] Coombes JL, Charsar BA, Han SJ, Halkias J, Chan SW, Koshy AA, et al. Motile invaded neutrophils in the small intestine of *Toxoplasma gondii*-infected mice reveal a potential mechanism for parasite spread. Proc Natl Acad Sci U S A 2013;110:E1913-22.

[7] Gregg B, Taylor BC, John B, Tait-Wojno ED, Girgis NM, Miller N, et al. Replication and distribution of *Toxoplasma gondii* in the small intestine after oral infection with tissue cysts. Infect Immun 2013;81:1635-43.

[8] Dubey JP. Bradyzoite-induced murine toxoplasmosis: stage conversion, pathogenesis, and tissue cyst formation in mice fed bradyzoites of different strains of *Toxoplasma gondii*. J Eukaryot Microbiol 1997;44:592-602.

[9] Barragan A, Brossier F, Sibley LD. Transepithelial migration of *Toxoplasma gondii* involves an interaction of intercellular adhesion molecule 1 (ICAM-1) with the parasite adhesin MIC2. Cell Microbiol 2005;7:561-8.

[10] Krug SM, Gunzel D, Conrad MP, Lee IF, Amasheh S, Fromm M, et al. Charge-selective claudin channels. Ann N Y Acad Sci 2012;1257:20-8.

[11] Chiba H, Osanai M, Murata M, Kojima T, Sawada N. Transmembrane proteins of tight junctions. Biochim Biophys Acta 2008;1778:588-600.

[12] Al-Sadi R, Khatib K, Guo S, Ye D, Youssef M, Ma T. Occludin regulates macromolecule flux across the intestinal epithelial tight junction barrier. Am J Physiol Gastrointest Liver Physiol 2011;300:G1054-64.

[13] Wong V. Phosphorylation of occludin correlates with occludin localization and function at the tight junction. Am J Physiol 1997;273:C1859-67.

[14] Raleigh DR, Boe DM, Yu D, Weber CR, Marchiando AM, Bradford EM, et al. Occludin S408 phosphorylation regulates tight junction protein interactions and barrier function. J Cell Biol 2011;193:565-82.

[15] Bonazzi M, Cossart P. Impenetrable barriers or entry portals? The role of cell-cell adhesion during infection. J Cell Biol 2011;195:349-58.

[16] Dalton JE, Cruickshank SM, Egan CE, Mears R, Newton DJ, Andrew EM, et al. Intraepithelial gammadelta+ lymphocytes maintain the integrity of intestinal epithelial tight junctions in response to infection. Gastroenterology 2006;131:818-29.

[17] Weight CM, Carding SR. The protozoan pathogen *Toxoplasma gondii* targets the paracellular pathway to invade the intestinal epithelium. Ann N Y Acad Sci 2012;1258:135-42.

[18] Bens M, Bogdanova A, Cluzeaud F, Miquerol L, Kerneis S, Kraehenbuhl JP, et al. Transimmortalized mouse intestinal cells (m-ICc12) that maintain a crypt phenotype. Am J Physiol 1996;270:C1666-74.

[19] Quaroni A, Wands J, Trelstad RL, Isselbacher KJ. Epithelioid cell cultures from rat small intestine. Characterization by morphologic and immunologic criteria. The Journal of cell biology 1979;80:248-65.

[20] Gubbels MJ, Li C, Striepen B. High-throughput growth assay for *Toxoplasma gondii* using yellow fluorescent protein. Antimicrob Agents Chemother 2003;47:309-16.

[21] Bamforth SD, Kniesel U, Wolburg H, Engelhardt B, Risau W. A dominant mutant of occludin disrupts tight junction structure and function. J Cell Sci 1999;112 (Pt 12):1879-88.

[22] Djurkovic-Djakovic O, Djokic V, Vujanic M, Zivkovic T, Bobic B, Nikolic A, et al. Kinetics of parasite burdens in blood and tissues during murine toxoplasmosis. Exp Parasitol 2012;131:372-6.

[23] Hill RD, Su C. High tissue burden of *Toxoplasma gondii* is the hallmark of acute virulence in mice. Vet Parasitol 2012;187:36-43.

[24] Dubey JP. Re-examination of resistance of *Toxoplasma gondii* tachyzoites and bradyzoites to pepsin and trypsin digestion. Parasitology 1998;116 (Pt 1):43-50.

[25] Bonametti AM, Passos JN, Koga da Silva EM, Macedo ZS. Probable transmission of acute toxoplasmosis through breast feeding. J Trop Pediatr 1997;43:116.

[26] Wood SR, Zhao Q, Smith LH, Daniels CK. Altered morphology in cultured rat intestinal epithelial IEC-6 cells is associated with alkaline phosphatase expression. Tissue & cell 2003;35:47-58.

[27] Morisaki JH, Heuser JE, Sibley LD. Invasion of *Toxoplasma gondii* occurs by active penetration of the host cell. J Cell Sci 1995;108 (Pt 6):2457-64.

[28] Fanning AS, Jameson BJ, Jesaitis LA, Anderson JM. The tight junction protein ZO-1 establishes a link between the transmembrane protein occludin and the actin cytoskeleton. J Biol Chem 1998;273:29745-53.

[29] Blasig IE, Winkler L, Lassowski B, Mueller SL, Zuleger N, Krause E, et al. On the self-association potential of transmembrane tight junction proteins. Cell Mol Life Sci 2006;63:505-14.

[30] Nusrat A, Brown GT, Tom J, Drake A, Bui TT, Quan C, et al. Multiple protein interactions involving proposed extracellular loop domains of the tight junction protein occludin. Mol Biol Cell 2005;16:1725-34.

[31] Boyle EC, Brown NF, Finlay BB. *Salmonella enterica* serovar *Typhimurium* effectors SopB, SopE, SopE2 and SipA disrupt tight junction structure and function. Cell Microbiol 2006;8:1946-57.

[32] Muza-Moons MM, Schneeberger EE, Hecht GA. Enteropathogenic *Escherichia coli* infection leads to appearance of aberrant tight junctions strands in the lateral membrane of intestinal epithelial cells. Cell Microbiol 2004;6:783-93.

[33] Black MW, Boothroyd JC. Lytic cycle of *Toxoplasma gondii*. Microbiol Mol Biol Rev 2000;64:607-23.

[34] Speer CA, Dubey JP. Ultrastructural differentiation of *Toxoplasma gondii* schizonts (types B to E) and gamonts in the intestines of cats fed bradyzoites. Int J Parasitol 2005;35:193-206.

[35] Lavine MD, Arrizabalaga G. Induction of mitotic S-phase of host and neighboring cells by *Toxoplasma gondii* enhances parasite invasion. Mol Biochem Parasitol 2009;164:95-9.

[36] Denney CF, Eckmann L, Reed SL. Chemokine secretion of human cells in response to Toxoplasma gondii infection. Infect Immun 1999;67:1547-52.

[37] Dolowschiak T, Chassin C, Ben Mkaddem S, Fuchs TM, Weiss S, Vandewalle A, et al. Potentiation of epithelial innate host responses by intercellular communication. PLoS Pathog 2010;6:e1001194.

[38] Kasper CA, Sorg I, Schmutz C, Tschon T, Wischnewski H, Kim ML, et al. Cell-cell propagation of NF-kappaB transcription factor and MAP kinase activation amplifies innate immunity against bacterial infection. Immunity 2010;33:804-16.

[39] Mineo JR, McLeod R, Mack D, Smith J, Khan IA, Ely KH, et al. Antibodies to *Toxoplasma gondii* major surface protein (SAG-1, P30) inhibit infection of host cells and are produced in murine intestine after peroral infection. J Immunol 1993;150:3951-64.

[40] Debierre-Grockiego F, Niehus S, Coddeville B, Elass E, Poirier F, Weingart R, et al. Binding of *Toxoplasma gondii* glycosylphosphatidylinositols to galectin-3 is required for their recognition by macrophages. J Biol Chem 2010;285:32744-50.

[41] Saouros S, Edwards-Jones B, Reiss M, Sawmynaden K, Cota E, Simpson P, et al. A novel galectin-like domain from *Toxoplasma gondii* micronemal protein 1 assists the folding, assembly, and transport of a cell adhesion complex. J Biol Chem 2005;280:38583-91.

[42] Carruthers VB, Hakansson S, Giddings OK, Sibley LD. *Toxoplasma gondii* uses sulfated proteoglycans for substrate and host cell attachment. Infect Immun 2000;68:4005-11.

[43] Jacquet A, Coulon L, De Neve J, Daminet V, Haumont M, Garcia L, et al. The surface antigen SAG3 mediates the attachment of *Toxoplasma gondii* to cell-surface proteoglycans. Mol Biochem Parasitol 2001;116:35-44.

[44] Monteiro VG, Soares CP, de Souza W. Host cell surface sialic acid residues are involved on the process of penetration of *Toxoplasma gond*ii into mammalian cells. FEMS Microbiol Lett 1998;164:323-7.

[45] Wong V, Gumbiner BM. A synthetic peptide corresponding to the extracellular domain of occludin perturbs the tight junction permeability barrier. J Cell Biol 1997;136:399-409.

[46] Lacaz-Vieira F, Jaeger MM, Farshori P, Kachar B. Small synthetic peptides homologous to segments of the first external loop of occludin impair tight junction resealing. J Membr Biol 1999;168:289-97.

[47] Veiga E, Guttman JA, Bonazzi M, Boucrot E, Toledo-Arana A, Lin AE, et al. Invasive and adherent bacterial pathogens co-Opt host clathrin for infection. Cell Host Microbe 2007;2:340-51.

Figure Legends

Figure 1: *T. gondii* localizes to epithelial cellular junctions before paracellular transmigration and/or infection. (A) Polarized m-IC_{c12} cultured on cell inserts were exposed to YFP-*T. gondii* for 2 h and stained for β-catenin (red). Arrows represent cells with parasites clustered around the lateral cell edge. Images are representative of those obtained from more than ten experiments with replicates. Scale bar = 10 µm. Further evidence for lateral localization of parasites was provided by scanning electron microscopy; visualized parasites clustered around cell edges as highlighted in blue (B). Scale bar = 2 µm. Parasites were seen penetrating the epithelial cells via the paracellular pathway (white arrow) as indicated by staining with occludin (red, C), β-catenin and surface carbohydrates (red and blue respectively, D), and, by transmission electron microscopy (E). TJ, tight junction; Tg, *T. gondii*; A, apical surface. Scale bar = 20 µm for (C and D) and 500 nm for (E). Experiments were carried out once with biological replicates for SEM and TEM. (F) Parasite transmigration across polarized monolayers was quantified by sampling the basal compartment for YFP-parasites after their addition to the apical compartment, using flow cytometry. (G) Intracellular parasites are contained within a parasitophorous vacuole appearing as a white halo surrounding the parasite (arrow) following H&E staining. Scale bar = 20 µm. (H) Supernatant from IECs, cultured in six well dishes and exposed to 1.5 x 10^6 parasites for 24 h, were assayed for the presence of cytokines using a bead array. Data represents three independent experiments with biological replicates. *** P <0.0001. (I-K) 2-Photon-microscope live imaging of IEC-6 monolayers (red) exposed to *T.gondii* (green) (See Video S1). Sequential frames from Video S1 show a transmigrating parasite targeting the epithelial cellular junction (white arrows). Following initial localization to the cellular junction (I), the parasite re-orientates (J) and enters the paracellular junction (K). A static intracellular parasite is clearly visible (White arrowheads). Corresponding YZ images show the parasite (marked *) localizes above the epithelial cellular junction (I'), re-orientates and moves between cells in the paracellular junction (J') and transmigrates through the epithelium (K'). The paracellular junction region is visible as a

non-stained space between cells (red). Images are representative of those obtained from two experiments with replicates. Scale bar = 5 µm.

Figure 2: *T. gondii* alters the distribution of occludin. (A-E) m-IC_{c12} cells grown on inserts were exposed to either media alone (A) or with parasites for 0.5 h (B), 2 h (C), 6 h (D) or 24 h (E), prior to staining with anti-occludin antibodies (red). A'-E' represents XZ images of corresponding XY optical slide images. Scale bar = 20 µm. Images are representative of those collected from over ten experiments with biological replicates. (F) Image quantification was used to assess occludin distribution across membrane and cytoplasmic cellular compartments as well as total cellular levels of occludin (G) prior and post exposure to parasites. The graphs represent image quantification of between 30 and 90 cells across 3 to 10 independent experiments using Image J. ** = $P<0.002$ and $P<0.0001$ comparing with no exposure to parasites.

Figure 3: *T. gondii* does not globally affect junctional proteins or epithelial barrier function. (A) m-IC_{c12} cells were stained for claudin-2, ZO-1 or β-catenin, pre- and post-infection (2 h or 6 h) with live parasites. Scale bar = 20 µm. Results are representative of 3 or more independent experiments with replicates. (B) Changes in barrier function were assessed by measuring TEER in response to parasites after 2 h exposure. The data shown represents results from seven separate determinations with biological replicates. $P = 0.2$. (C) Epithelial permeability was assessed by measuring transmigration of FITC-dextran across epithelial cells cultured in transwells prior and after 2 h exposure to parasites. The data shown represents results from three separate determinations with biological replicates. $P = 0.4$.

Figure 4: *T. gondii* co-localizes with occludin during infection and transmigration. (A) m-IC_{c12} cells were exposed to *T. gondii* (green) for 2 h and stained for occludin (red) with co-localization (arrows) appearing yellow. Magnified images of individual cells show a

transmigrating parasite (B) and an internalized parasite (C). (D) and (E) highlight occludin-parasite co-localization in the XZ plane. Anti-occludin antibodies do not stain the parasites in isolation (F). By 24 h post-infection occludin is redistributed intracellularly (G) with multiple parasites residing within infected cells (H). (I) shows the merged (G) and (H) images. Scale bar = 20 µm. Images are representative of those from three to ten independent experiments with biological replicates.

Figure 5: Reduction of occludin expression impacts on parasite infection and transmigration. m-IC_{c12} were cultured on plastic to 80% confluency before adding occludin small interfering (siRNA) or non-silencing siRNA (scRNA). (A) Reduction of occludin was determined by immunoblotting 48 h post-transfection. Immunoblots were analyzed by densitometry with the values graphically shown, representing the levels of occludin in siRNA cell lysates relative to non-silenced siRNA-treated cells. Data is a representative from one of three independent experiments. Barrier function of siRNA-treated cells was assessed by measuring TEER (B, P = 0.5673) and permeability to FITC-dextran at 2 h post-parasite infection (C, P = 0.83). A value of 100% represents no change in TEER. The data shown represents results from three or more independent experiments with replicates. (D and E) m-IC_{c12} cells on coverslips were H&E stained to visualize and count parasites. Parasites that did not appear to have a white halo, indicative of intracellular parasitophorous vacuoles containing parasites, were assumed to be attached but not intracellular (D). Data represents results from four independent experiments with biological replicates. * P = 0.0129. (E) Infectivity of siRNA-treated cells was determined by counting the number of H&E-stained cells infected with parasites. Between 48 and 73 fields of view were recorded for each treatment with the data shown representing the percentage of cells infected compared to non-treated cells from four independent experiments with replicates. * P = 0.0191. (F) The ability of parasites to transmigrate occludin-reduced cells was determined in transwell cultures using flow cytometry to visualize and quantify parasites

appearing in the basal compartment 2 h post-infection. The data shown represents results from three independent experiments with biological replicates. * P = 0.0157. (G) To establish that there were no discrepancies in the initial number of parasites incubated with the cells, parasites were collected and counted from the apical chamber of cells grown on transwell inserts. Data represents results from three independent experiments with biological replicates. P = 0.9705. (H-K) Cells grown on inserts for 11 days were treated with either occludin-specific siRNA or non-specific siRNA. (H) Cells were visualized for the presence of occludin 48 h post-transfection. Cells were also visualized for changes in occludin distribution following exposure to *T. gondii* for 2 h. Images are representative of 4 independent experiments. (I-K) Other junctional proteins were not affected by the reduction of occludin. Images represent data from three or more independent experiments. Scale bar = 20 μm.

Figure 6: Recombinant murine occludin peptides. (A) Occludin peptides corresponding to amino acids 191-241 (full length ECL2), 85-241 (full length ECL1-ECL2) and 261-521 (full length C-terminus) were generated as described in the Materials and Methods section. Amino acid number and distribution across the N terminus, transmembrane domains (TM), extracellular loops (ECL), intracellular loop (IL) and C-terminus were adapted from www.zonapse.net/occludin. (B) Peptide purity was assessed by immunoblotting using commercial anti-occludin antibodies.

Figure 7: *T. gondii* binds the extracellular loops of occludin. (A) The apical surface of IEC-6 weas exposed for 2 h with either *T. gondii* (control) or *T. gondii* pre-incubated with 2μM recombinant occludin peptides and were subsequently stained with H&E to visualize and count parasites. Parasites that did not have a white halo, indicative of intracellular parasitophorous vacuoles containing parasites, were assumed to be attached but not intracellular. Between 6 and

12 fields of view were recorded for each treatment with the data shown representing the normalized change in parasite attachment when parasites were pre-incubated with recombinant occludin peptides compared to non-treated parasites (control). Data shown is from three independent experiments with replicates. *** = P<0.001 **** = P<0.0001. (B and C) In a solid-phase parasite-occludin binding assay YFP-parasites were incubated with HIS-tagged ECL1+ECL2, ECL1, ECL2, or C-terminus fragments of murine occludin immobilized to individual wells of a chamber slide with bound parasites visualized by UV microscopy. Wells containing a HIS-tagged mCherry recombinant protein and/or binding buffer alone (Control) were used as controls. (B) Binding of parasites to occludin peptides was quantified by fluorescent pixel counts using 6-12 fields of view per well (*= P<0.05 ** = P<0.01). Data represents three independent experiments with replicates. (C) The fluorescent images shown are representative of those obtained from three experiments with replicates. Scale bar = 20 µm.

Figure 1

Click here to download high resolution image

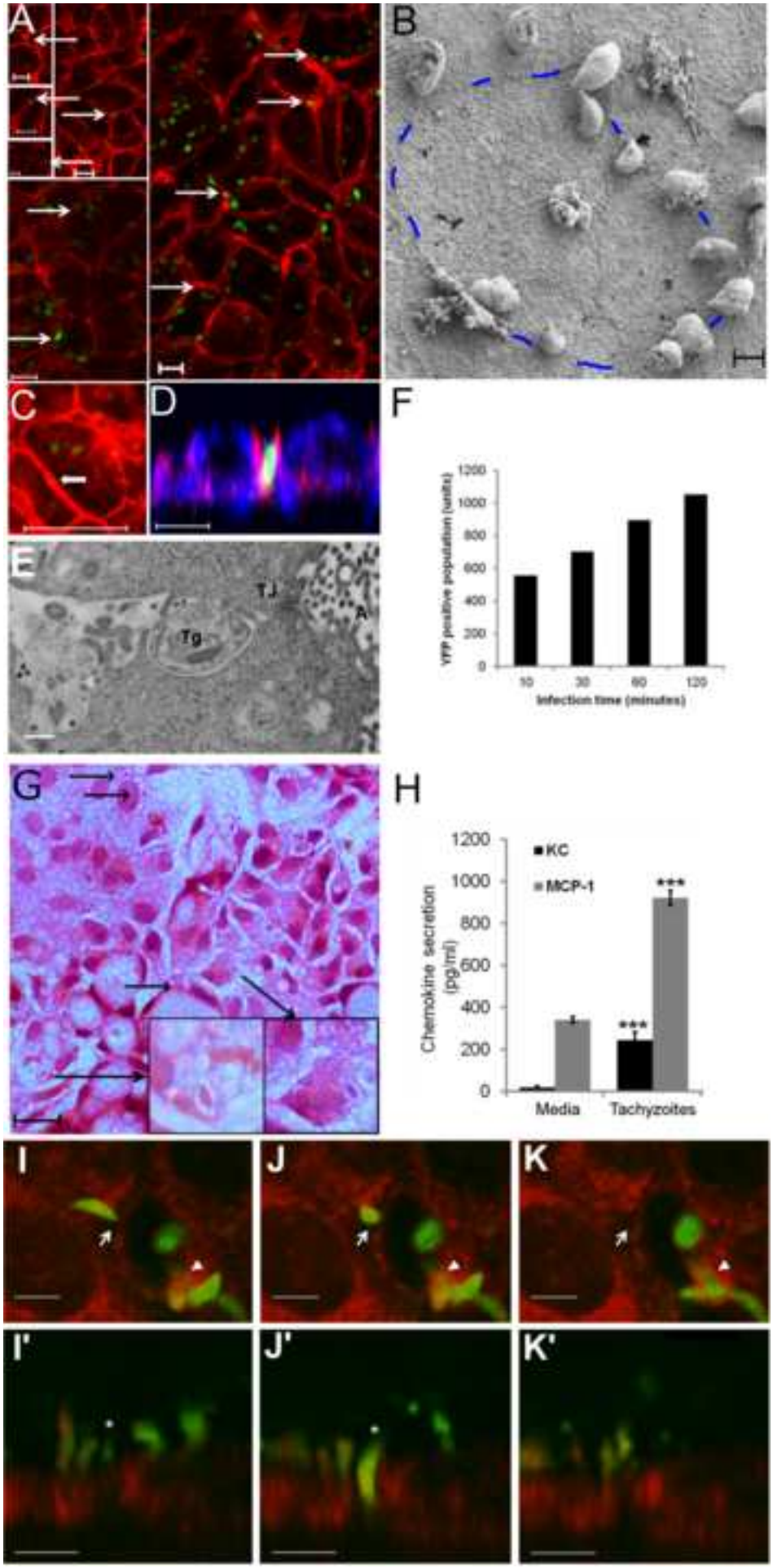

Figure 2

Click here to download high resolution image

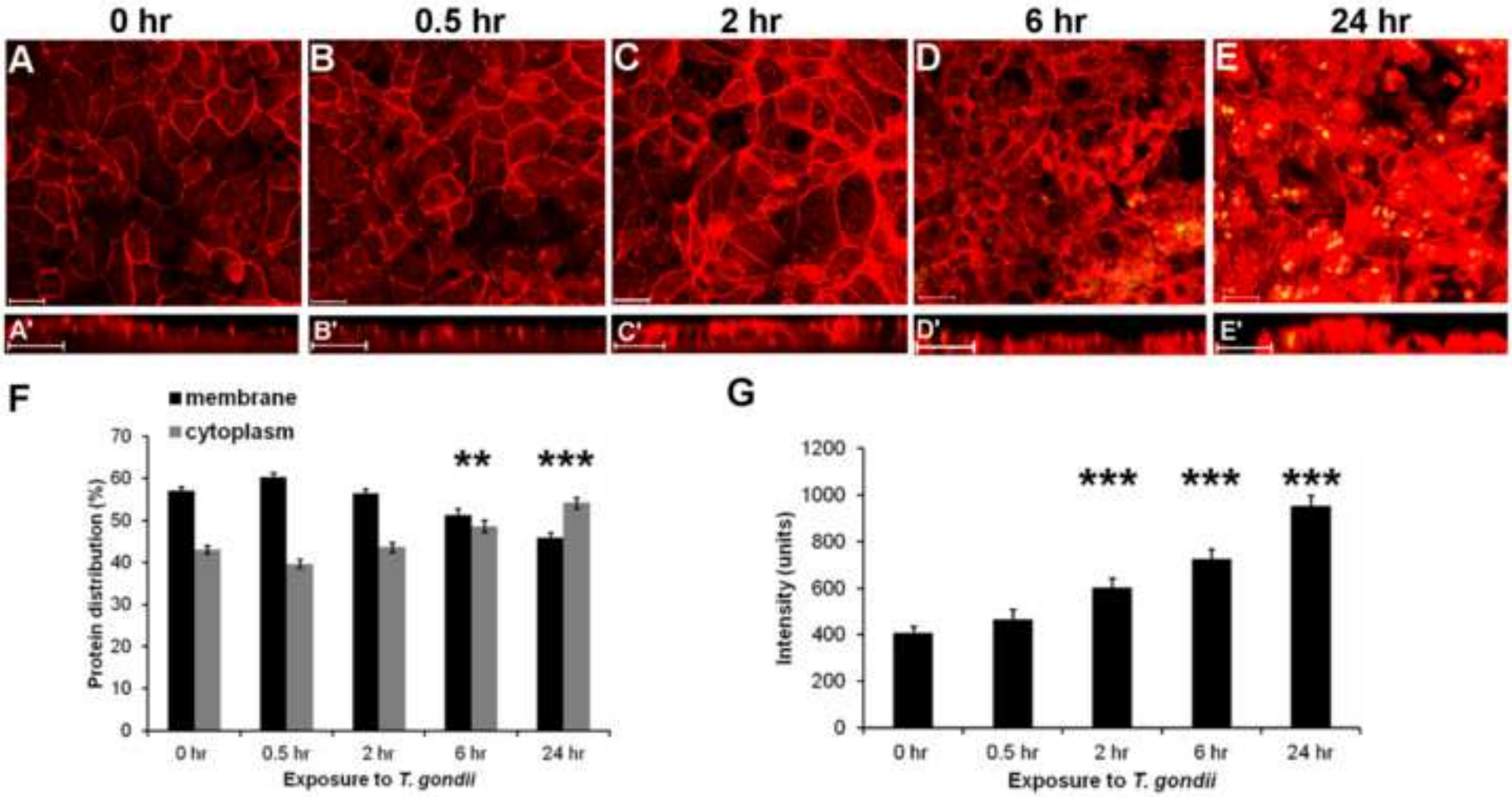

Figure 3
Click here to download high resolution image

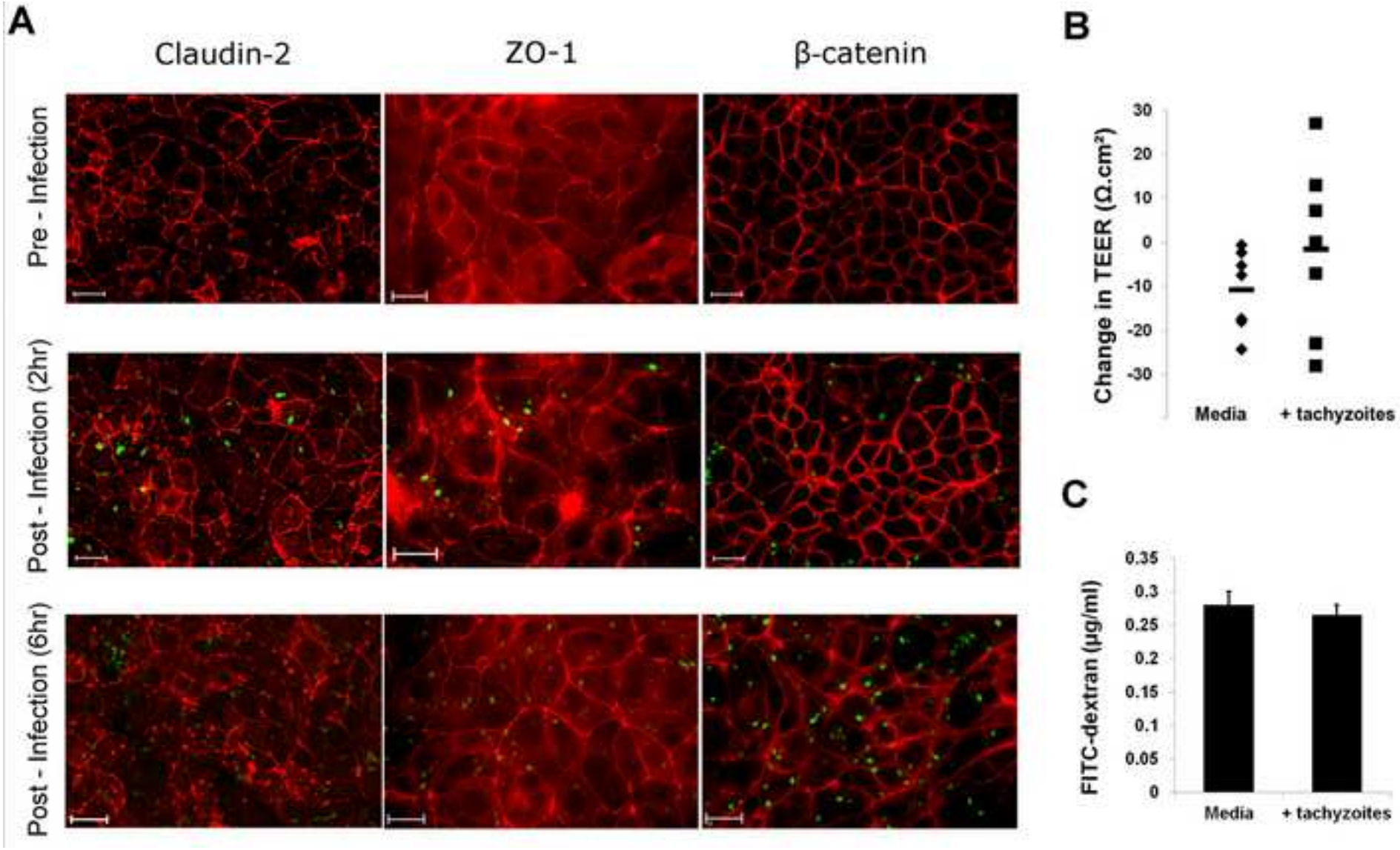

Figure 4

Click here to download high resolution image

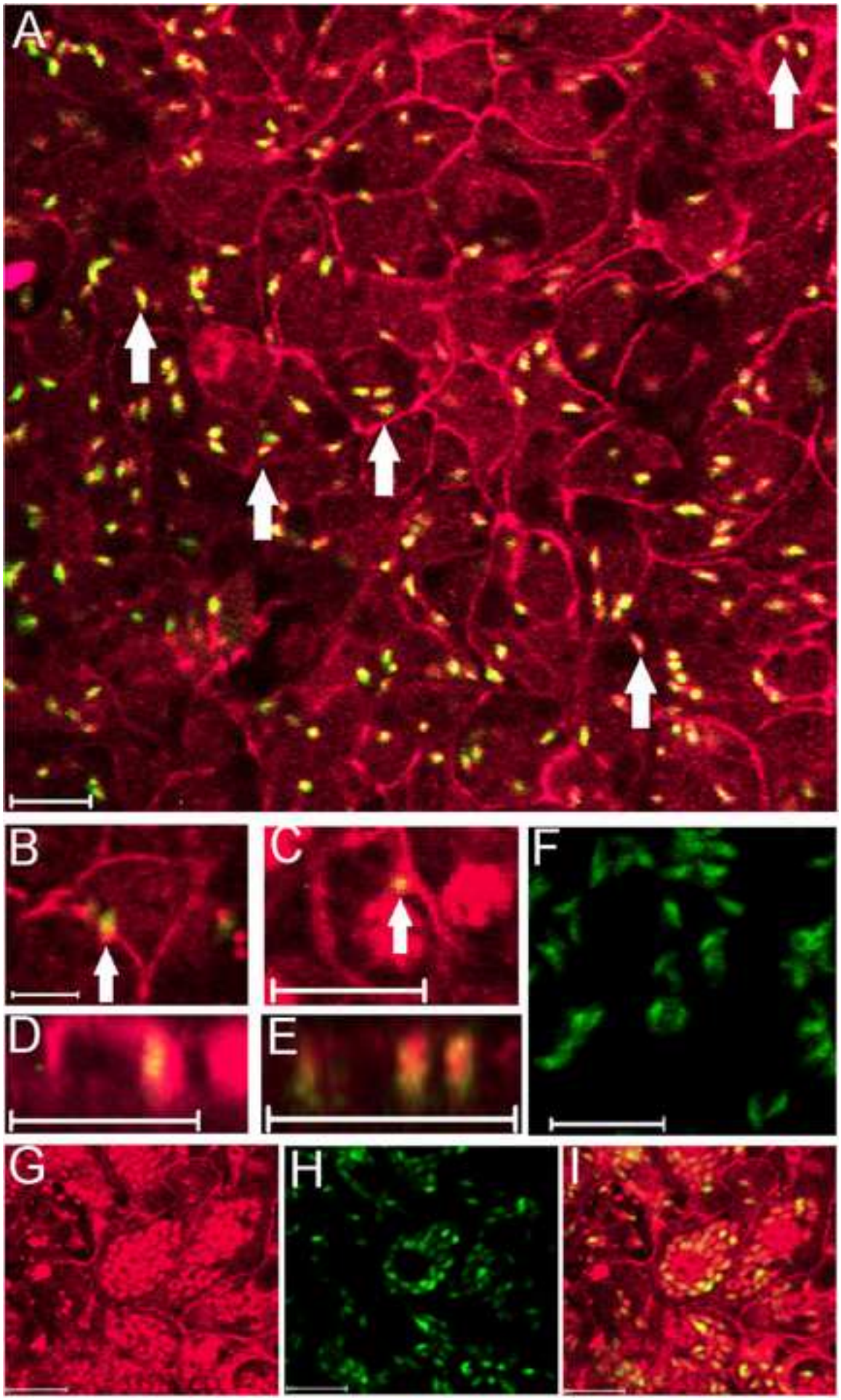

Figure 5

Click here to download high resolution image

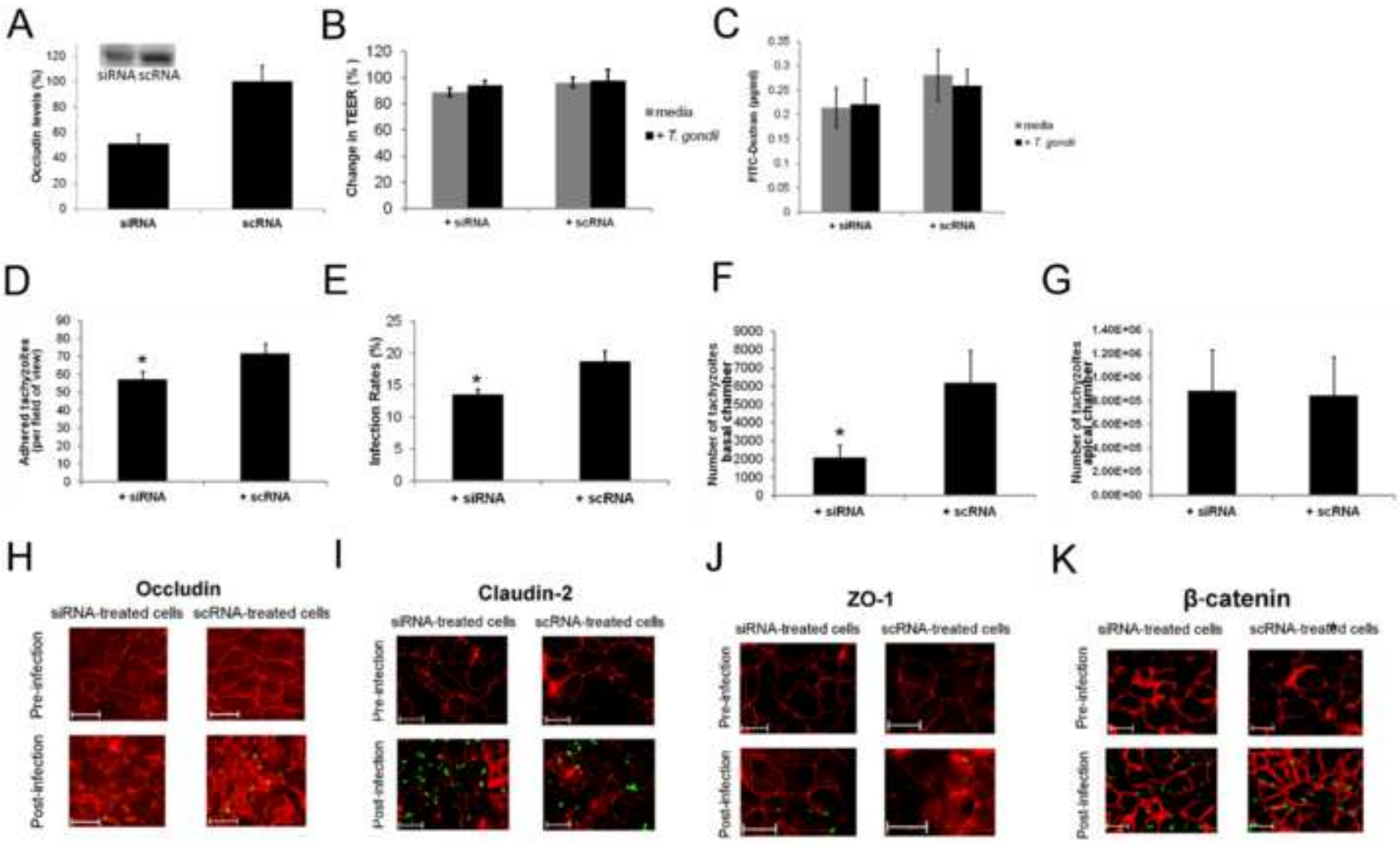

Figure 6

Click here to download high resolution image

Figure 7

Click here to download high resolution image

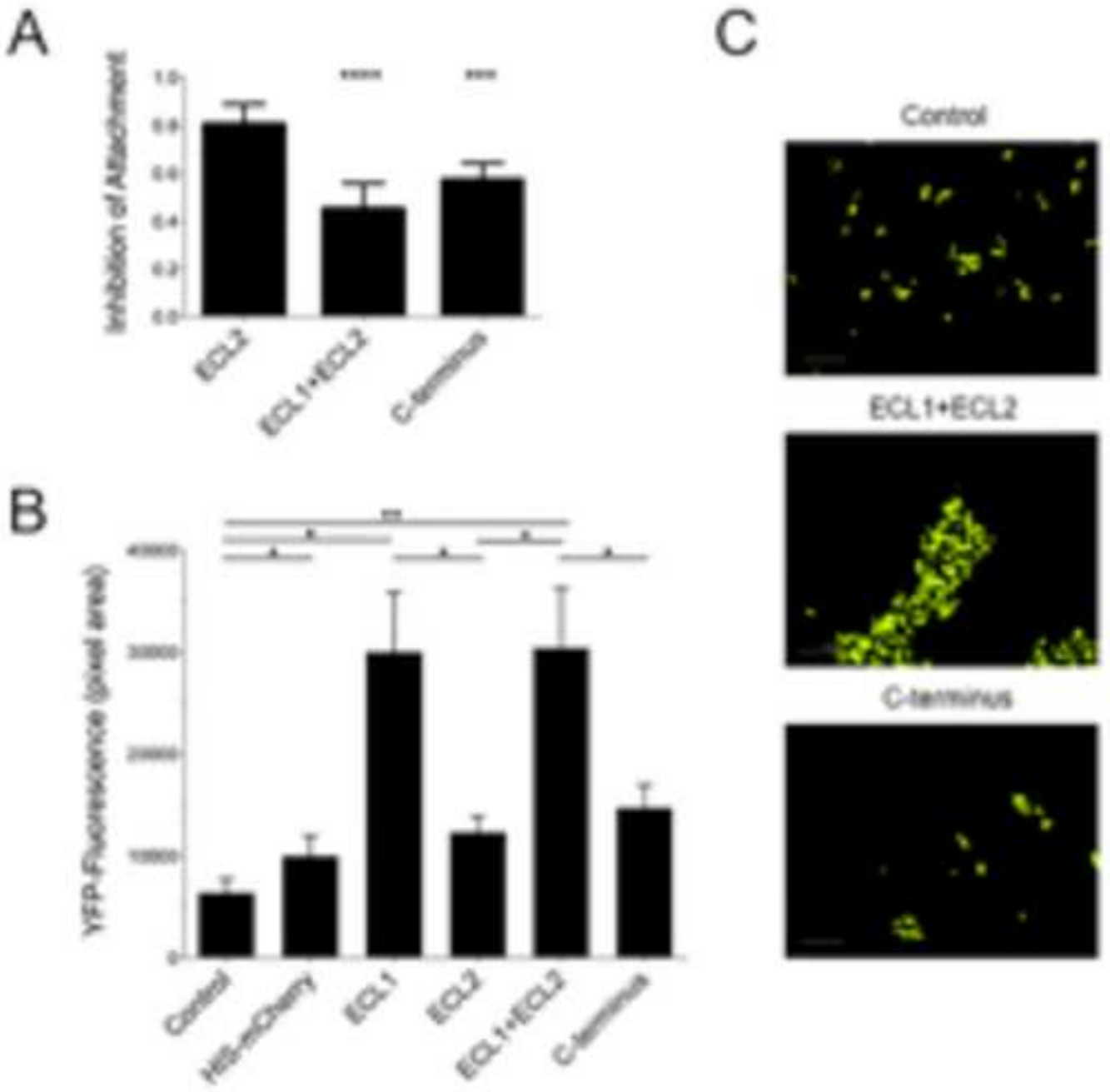

19th June 2015

Manuscript Reference No: MICINF-D-15-00103

Dear Dr. Denkers,

Thank you very much for reviewing our manuscript. We have read through the comments and recognize the points raised are important to address. Below we have detailed our response to each of the reviewer's comments:

Underlining highlights corrections made to the text.

Reviewer #1:

1. The authors show that parasites cluster around cellular junctions and use a paracellular route. Taken together, this is convincing, however the information contained in the TEM images in fig.1B and 1E needs to be better explained to the reader. Cell edges (1B) and intracellular structures (1E) are not very clear.

Response: We appreciate that a better explanation was required and have adjusted the text accordingly.

2. Redistribution of occludin (fig 2). It is difficult to evaluate the redistribution of occludin as no information is provided in M&M or figure legends on what focal planes and cut-offs were utilized to quantify fluorescence in "membrane" or "cytoplasm". As a putative direct interaction of the parasite with occludin is central to the manuscript, this should be clarified. The redistribution of occludin should also be related to other markers studied in fig 3 (claudin-2, zonula occludens-1, beta-catenin). The authors state that "distribution of other junctional proteins was not obviously altered" but that "slight differences may be attributed to indirect effects". This needs to be addressed and clarified.

Response: We agree that clarification of methods would improve the understanding of how our data was collected and have made changes to address this comment. We have also improved our description of the text relating to indirect effects of other tight junction proteins.

3. The evidence that tachyzoites co-localize or are in close vicinity of occludin when transmigrating is convincing (fig 4). However, the evidence of tachyzoite interaction with occludin (fig 6) is indirect. Have the authors tried to block transmigration with the generated occludin peptides? In theory, the peptides should compete with binding of tachyzoites to native occludin and thus could add evidence to the proposed interaction and also add functionality to this manuscript.

Response: We have included data from an epithelial cell attachment and invasion assay using occludin peptides. Whilst it was not possible due to technical reasons (difficulty of producing sufficient amounts of ECL1) to include all of the peptides used in the parasite-binding assay as in this invasion assay, the data does show that the ECL1+ECL2 peptide significantly reduce the ability of parasites to attach and invade epithelial cells whereas the ECL2 peptide has no discernable effect (Figure 7A). This is consistent with the occuldin peptide-parasite binding assay data (Figure 7B) and that parasite binding to occludin principally involves the ECL1 region of the tight junction protein.

4. As the tachyzoite stage is not the natural stage for oral infection, stating (page 11) that tachyzoites are infective via the oral route without further explanation of the experimental setups or a statement that bradyzoites/oocysts are the "natural" infection stages could be misleading to some readers.

Response: We have expanded our text and included the reviewer's suggestion to state the natural infection routes.

Reviewer #2:

The manuscript by Weight et al describes the involvement of the tight junction protein occludin in the transmigration of Toxoplasma gondii through the epithelial barrier. Were also other proteins except ZO-1, claudin-2 and beta-catenin used as controls? Why were these selected? Immortalized cell lines are known to lose their characteristics therefore primary cells should be applied as controls.

Response: We also used a second control tight junction protein but as the results were the same as with the first control protein we decided that this information was not necessary to show. However, we acknowledge that the reasons we chose Claudin-2, beta catenin and ZO-1 are not fully stated. This has now been incorporated in the text. While the authors agree that for any study primary cells could be used as controls, this is technically very challenging due the difficulty of maintaining fully differentiated primary cells in vitro for prolonged periods of time. Our study was conducted on cell lines that have been fully characterized previously to show exceptional and important characteristics found in vivo. It is also important to note that in contrast to the large number of colonic epithelial cell lines available, the two epithelial cell lines we have used in our study are the only ones available, irrespective of the species of origin, that originate from and are representative of those cells of the small intestine.

I hope that the revisions we have made are acceptable to the reviewers and that the manuscript can now be viewed as meeting the criteria for publication in *Microbes and Infection*.

Sincerely,

Simon R. Carding
(on behalf of the authors)

Video

Click here to download e-component: VIDEO S1.avi

Video Still

Click here to download high resolution image